Dynamic Light Scattering

Experiment DLS

University of Florida — Department of Physics
PHY4803L — Advanced Physics Laboratory

Objective

A HeNe laser beam incident on a sample of micron-sized spheres suspended in water scatters into a random pattern of spots of varying size, shape, and intensity. The pattern results from the coherent superposition of the outgoing waves scattered from the spheres. Because the spheres are in constant Brownian motion, the pattern randomly changes in time. A photodetector is placed in the pattern and the random fluctuations in the light intensity are measured and analyzed. The signal's autocorrelation function and power spectrum are computed and used to verify the Brownian motion and determine the spheres' diameter.

References

Clark, Lancek, and Benedek *A Study of Brownian Motion Using Light Scattering*, Amer. J. of Phys. **38**, 575 (1970).

Daniel T. Gillespie *The mathematics of Brownian motion and Johnson noise*, Amer. J. of Phys. **64** 225 (1996).

Daniel T. Gillespie *Fluctuation and dissipation in Brownian motion*, Amer. J. of Phys. **61** 1077 (1993).

Introduction

Scattering experiments can provide a wealth of detailed information about the structural and dynamical properties of matter. Dynamic light scattering, in particular, has important applications in particle and macromolecule sizing and brings in another important topic in physics: Brownian motion. We begin with a brief discussion of Brownian motion and dynamic light scattering before describing the apparatus and measurements.

Brownian motion

Brownian motion refers to the random diffusive motion of microscopic particles suspended in a liquid or a gas. This motion was first studied in detail by Robert Brown in 1827 when he observed the motion of pollen grains in water through his microscope. More systematic studies found the motion depends on particle size, liquid viscosity and temperature and around 1905 Albert Einstein and M. Smoluchowski independently connected Brownian motion to the kinetic theory.

Before considering Brownian motion, let's first recall certain aspects of the kinetic theory for the molecules of the suspension liquid. These molecules are in constant thermal motion having a Maxwell-Boltzmann velocity distribution. This distribution gives the proba-

bility for the molecule to have a velocity between v_x and $v_x + dv_x$ as

$$dP(v_x) = \sqrt{\frac{m}{2\pi k_B T}} e^{-mv_x^2/2k_B T} dv_x \quad (1)$$

where m is the molecular mass, k_B is Boltzmann's constant, and T is the temperature. Of course, analogous expressions apply to the y- and z-components of velocity. Equation 1 is a Gaussian probability distribution with a mean of zero and a variance of $k_B T/m$.

We will use a shorthand notation

$$N(\mu, \sigma^2) \quad (2)$$

to express a Gaussian distribution of mean μ and variance σ^2 and, for example, the equation

$$v_x = N\left(0, \frac{k_B T}{m}\right) \quad (3)$$

will be a shorthand notation expressing that the x-component of velocity for a suspension molecule is a sample from the probability distribution of Eq. 1.

The *equipartition theorem* states that each degree of freedom must have an average energy of $k_B T/2$. For the translational degree of freedom in the x-direction this implies:

$$\frac{1}{2}m\left\langle v_x^2 \right\rangle = \frac{1}{2}k_B T \quad (4)$$

where the angle brackets $\langle\rangle$ indicate taking an average over the appropriate probability distribution. For example, with the Maxwell-Boltzmann probability distribution for v_x (Eq. 1),

$$\left\langle v_x^2 \right\rangle = \sqrt{\frac{m}{2\pi k_B T}} \int_{-\infty}^{\infty} v_x^2 e^{-mv_x^2/2k_B T} dv_x \quad (5)$$

which gives $\left\langle v_x^2 \right\rangle = k_B T/m$, and is clearly consistent with Eq. 4.

Numerical solutions to the motion of a particle typically begin with Newton's second law cast in the form:

$$d\mathbf{r}(t) = \mathbf{v}(t)dt \quad (6)$$
$$d\mathbf{v}(t) = \frac{1}{M}\mathbf{F}(t)dt \quad (7)$$

where M is the particle mass, $\mathbf{r}(t)$ is its position, $\mathbf{v}(t)$ is its velocity, and $\mathbf{F}(t)$ is the net force on the particle. One chooses some small but finite dt over which $\mathbf{r}(t)$ and $\mathbf{v}(t)$ can be assumed constant. $\mathbf{F}(t)$, which may depend on $\mathbf{r}$ and $\mathbf{v}$, is evaluated and the right sides of Eqs. 6 and 7 are calculated. With the left sides defined by

$$d\mathbf{r}(t) = \mathbf{r}(t+dt) - \mathbf{r}(t) \quad (8)$$
$$d\mathbf{v}(t) = \mathbf{v}(t+dt) - \mathbf{v}(t) \quad (9)$$

the right-side values are then added to the values $\mathbf{r}(t)$ and $\mathbf{v}(t)$ to obtain updated values $\mathbf{r}(t+dt)$ and $\mathbf{v}(t+dt)$ at a time dt later. Starting from given initial conditions for $\mathbf{r}(0) = \mathbf{r}_0$ and $\mathbf{v}(0) = \mathbf{v}_0$ at $t = 0$, the process is repeated to obtain future values for $\mathbf{r}(t)$ and $\mathbf{v}(t)$ at discrete intervals. As we will see, this modeling of the equations of motion is particularly appropriate for Brownian motion.

The motion is said to be *deterministic* when $\mathbf{F}(t)$ can be precisely determined from the values of $\mathbf{r}(t)$, $\mathbf{v}(t)$, and t. For example, in a collision between two particles with a known interaction (such as the Coulomb or gravitational force) $\mathbf{F}(t)$ is deterministic and the motion is quite predictable.[1]

For Brownian motion, $\mathbf{F}(t)$ arises from the continual collisions of suspension molecules against the particle. Each interaction with a suspension molecule during a collision delivers

---

[1]Deterministic does not always mean predictable. Some perfectly precise forms of $\mathbf{F}(t)$ lead to chaotic solutions that cannot be predicted far into the future at all.

an impulse to the particle

$$\mathbf{J}_i = \int \mathbf{F}_i(t)dt \qquad (10)$$

where $\mathbf{F}_i(t)$ is the force on the particle and the integral extends over the duration of the collision. The individual impulses $\mathbf{J}_i$ vary in size and direction depending on the speeds and angles involved in the collision. Velocities vary according to the Maxwell-Boltzmann distribution and average around 600 m/s for room temperature water. Collisions are short and frequent, occurring around 10^{19} times per second for a $1\,\mu$ particle in water. The randomness of the individual collisions leads to a net force that includes random components and the force and motion are said to be *stochastic.* The motion of a single particle is unpredictable and only probabilities or average behavior can be determined.

Because of the high collision frequency, we can choose a time interval dt short enough that $\mathbf{r}(t)$ and $\mathbf{v}(t)$ do not change significantly, yet long enough to include thousands of collisions. Over such an interval, the value of $\mathbf{F}(t)dt$ in Eq. 7 would properly be the sum of all impulses delivered during the interval dt

$$\mathbf{F}(t)dt = \sum_i \mathbf{J}_i \qquad (11)$$

With enough collisions, the *central limit theorem* can be used to draw important conclusions about the form of $\mathbf{F}(t)dt$ even though detailed knowledge of individual impulses is lacking.

The central limit theorem states that the sum of many random numbers will always be a Gaussian-distributed random number. More specifically, it states that if each of the individual random numbers are from a distribution (which need not be Gaussian) having a mean μ_i and variance σ_i^2, then the sum of N such random numbers will be a random number

from a Gaussian distribution of mean $\mu = N\mu_i$ and variance $\sigma^2 = N\sigma_i^2$.

Each cartesian component of $\mathbf{J}_i$ can be assumed to be a random number from some (unknown) distribution and thus the central limit theorem applies to each component of Eq. 11. Remember, $\mathbf{v}(t)$ and $\mathbf{r}(t)$ do not change significantly over the interval dt; the probability distributions for the components of $\mathbf{J}_i$ arise from the distribution of velocities for the suspension molecules and from the distribution of collision angles. Moreover, because the number of collisions N over a time interval dt will be proportional to dt, the central limit theorem implies that each component of $\mathbf{F}(t)dt$ will be a random number from a Gaussian distribution having a mean and variance proportional to dt.

Shortly after Einstein's work on the subject, Paul Langevin hypothesized that $\mathbf{F}(t)dt$ can be expressed

$$\mathbf{F}(t)dt = -\alpha\mathbf{v}(t)\,dt + \mathbf{F}^{(r)}(t)\,dt \qquad (12)$$

The viscous drag force $-\alpha\mathbf{v}$, opposite in direction and proportional to the velocity, had already been investigated by Stokes, who showed that the drag coefficient for a sphere of diameter d in a suspension of viscosity η is given by

$$\alpha = 3\pi\eta d \qquad (13)$$

$\mathbf{F}^{(r)}(t)$ is the random part of the collisional force, which Langevin successfully characterized and showed how it was responsible for Brownian motion.

Keeping in mind that any random number from a distribution with a mean μ and variance σ^2 can be considered as the sum of the mean and a zero-mean random number having a variance σ^2

$$N(\mu, \sigma^2) = \mu + N(0, \sigma^2) \qquad (14)$$

allows one to see how Eq. 12 is related to Eq. 11 and the central limit theorem. Each

cartesian component of the $-\alpha\mathbf{v}\,dt$ term in Eq. 12 is the mean of the sum in the central limit theorem applied to that component of Eq. 11. With the means accounted for by the $-\alpha\mathbf{v}\,dt$ term, each component of the $\mathbf{F}^{(r)}(t)dt$ term must be a zero-mean, Gaussian-distributed random number providing the random or distributed part of the central limit theorem.

After enough collisions, the probability distribution for the particle velocity must become independent of any initial velocity and equilibrate at the Maxwell-Boltzmann distribution.

Exercise 1 *Determine the room temperature rms velocities ($\sqrt{\langle v^2 \rangle}$) of water molecules and of $1\,\mu$ diameter spheres in water. Assume the spheres have the density of water.*

Of course, it is the random collisions with the suspension molecules that will establish the particle's velocity distribution. In the Langevin model, the $\mathbf{F}^{(r)}(t)\,dt$ term will be responsible for establishing it. The *fluctuation-dissipation theorem* describes how this happens and implies that over any interval dt

$$F_x^{(r)}(t)dt = N(0, 2\alpha k_B T\,dt) \qquad (15)$$

This equation also holds for the y and z-components. It specifies the variance of the random term in terms of the temperature of the suspension and the drag coefficient.

Note that the mean, or $-\alpha\mathbf{v}\,dt$ term, is proportional to dt as required by the central limit theorem. Note also that the random $\mathbf{F}^{(r)}(t)dt$ term also satisfies the theorem in that its variance is proportional to dt. Actually, these two proportionalities are required if Eqs. 6 and 7 are to give self-consistent solutions as the step size dt is varied.

Exercise 2 *When solving differential equations numerically, the time step dt must be*

chosen small enough that $\mathbf{r}(t)$ and $\mathbf{v}(t)$ make only small changes during the interval. However, dt must not be made too small because roundoff and other numerical errors occur with each step. Often, one looks at the numerical solutions for $\mathbf{r}(t)$ and $\mathbf{v}(t)$ as the step size dt is decreased, choosing a dt where there is little dependence on its size.

Why do the mean and variance of $\mathbf{F}\,dt$ have to be proportional to dt in order for the equations of motion to be self consistent? Your answer should take into account how the sum of two Gaussian random numbers behave (on average) and how $\mathbf{v}(t)$ (on average) would change over one interval dt or over two intervals half as long.

We will take initial conditions at $t = 0$ of $\mathbf{r}(0) = \mathbf{r}_0$ and $\mathbf{v}(0) = \mathbf{v}_0$. Thus, the solution will start with a well defined position and velocity. However, the nature of the stochastic force implies that the particle position and velocity for $t > 0$ will be probability distributions that change with time. The references show how to get them. Here, they are simply presented without proof.

With analogous solutions for the other two velocity components, the solution for $v_x(t)$ can be written

$$v_x(t) = N\left(v_{0x}e^{-t/\tau}, \frac{k_B T}{M}(1 - e^{-2t/\tau})\right) \quad (16)$$

where

$$\tau = \frac{M}{\alpha} \qquad (17)$$

As required at $t = 0$, Eq. 16 has the value $v_x(0) = N(v_{0x}, 0)$ (i.e., the sure value v_{0x}). And at $t = \infty$ it has the solution $v_x(\infty) = N(0, k_B T/M)$, i.e., the Maxwell-Boltzmann distribution. Keep in mind that $t = \infty$ is really $t \gg \tau$ and τ is a very short; for a $1\,\mu$ particle in water, $\tau \approx 50$ ns. Note how τ in Eq. 16 describes the exponential decay of any

initial velocity and (within a factor of two) the exponential approach to the equilibrium velocity distribution.

The probability distribution for the position $\mathbf{r}(t)$ is slightly more complicated. With analogous solutions for $y(t)$ and $z(t)$, the result can be expressed

$$x(t) = N(\mu_x, \sigma^2) \tag{18}$$

where

$$\mu_x(t) = x_0 + v_{x0}\tau(1 - e^{-t/\tau}) \tag{19}$$

and

$$\sigma^2(t) = \frac{2k_BT}{\alpha}\left[t - 2\tau(1 - e^{-t/\tau}) \right. \tag{20}$$
$$\left. + \frac{\tau}{2}(1 - e^{-2t/\tau})\right]$$

For a particle released from rest at the origin ($\mathbf{r}_0 = 0$, $\mathbf{v}_0 = 0$), the equilibrium position distribution then becomes

$$x(t) = N(0, \sigma^2) \tag{21}$$

where

$$\sigma^2 = \frac{2k_BTt}{\alpha} \tag{22}$$

Note that important result that the variance of the distribution grows linearly with time.

Recall that Eq. 21 means that the probability for the particle to have a x-displacement from x to $x + dx$ is given by

$$dP(x) = \frac{1}{\sqrt{2\pi\sigma^2}}e^{-x^2/2\sigma^2}dx \tag{23}$$

The probability for the particle's displacement to be in a volume element $dV = dx\,dy\,dz$ around a particular value of $\mathbf{r}$ is the product of three such distributions—one for each direction x, y and z. Using $r^2 = x^2 + y^2 + z^2$, the product becomes

$$dP(\mathbf{r}) = \frac{1}{(2\pi\sigma^2)^{3/2}}e^{-r^2/2\sigma^2}dV \tag{24}$$

Consider a large number N of particles placed at the origin at $t = 0$. According to Eq. 24, each will have the probability $dP(\mathbf{r})$ to be in the volume element dV located at that $\mathbf{r}$. Consequently, the number of particles in that volume element will be $NdP(\mathbf{r})$ and their number density would be given by $\rho(\mathbf{r}) = NdP(\mathbf{r})/dV$ or

$$\rho(\mathbf{r}, t) = \frac{N}{(2\pi\sigma^2)^{3/2}}e^{-r^2/2\sigma^2} \tag{25}$$

where the (implicit) time dependence arises because σ^2 grows linearly in time via Eq. 22.

The particles would spread according to Eq. 25 with Eq. 22 until they start to reach the container walls and would continue moving from regions of higher concentration to regions of lower concentration until they are uniformly distributed throughout the suspension. Fick's second law of diffusion describes how $\rho(\mathbf{r})$ will change in time.

$$\frac{d\rho}{dt} = D\nabla^2\rho \tag{26}$$

where D is the *diffusion constant* describing the speed of the diffusion process. Einstein realized how Fick's second law is related to Brownian diffusion and was the first to relate D to σ.

Exercise 3 *Show that $\rho(\mathbf{r}, t)$ satisfies Eq. 26 with*

$$\sigma^2 = 2Dt \tag{27}$$

Substituting Eq. 22 with Eq. 13 into Eq. 27 leads to the Stokes-Einstein relation

$$D = \frac{k_BT}{3\pi\eta d} \tag{28}$$

Exercise 4 *Eq. 27 says the width of the particle distribution increases with t. Qualitatively, this behavior is reasonable because with more time for the random Brownian motion, one*
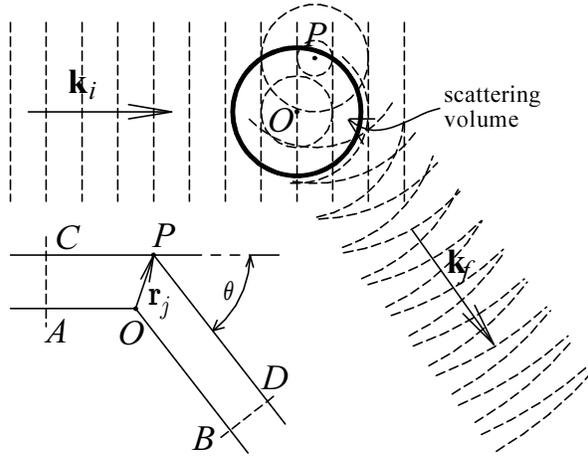
Figure 1: Upper figure: Coherent scattering. Incident plane wavefronts (dotted lines) traveling in the direction of wave vector $\mathbf{k}_i$ initiate scattered spherical wavefronts (dotted circles) from particles in the scattering volume. In the direction $\mathbf{k}_f$, where the detector will be placed, is shown scattered waves from two particles interfering. Lower figure: If the detector is far from the volume, the path length difference $\overline{CPD} - \overline{AOB}$ determines the phase of the electric field oscillations at the detector from the wave scattered from a particle at $\mathbf{r}_j$.

would expect the values of $\mathbf{r}$ to become more spread out. Explain in a similar qualitative way why the width of the distribution would be expected to increase with T and decrease with η and d as predicted by Eq. 28.

Dynamic light scattering

Consider first the idealized scattering problem shown schematically at the top of Fig. 1. A monochromatic plane wave travels in a transparent liquid extending throughout all of space. Identical micron-sized spheres undergo Brownian motion within a small volume V and scatter the incident wave. Far from the volume, the radiation scattered from each sphere

is well approximated by an outgoing spherical wave, and the electric field at the detector will be the sum of the spherical waves from all spheres.

The outgoing spherical wave from a single stationary sphere would produce a simple sinusoidal variation of the electric field strength at the detector

$$E_0 e^{i(\phi - \omega_0 t)} \tag{29}$$

where complex notation is used in which physical quantities are obtained as the real part of complex expressions, e.g., the real electric field strength above would be $E_0 \cos(\phi - \omega_0 t)$. The angular frequency of oscillations ω_0 is the same as that of the incident plane wave. E_0, the amplitude of the oscillation at the detector, is proportional to the amplitude of the incident plane wave, and depends on various properties of the sphere and the medium (e.g., their polarizability) as well as the incident wave's polarization and the scattering angle. Also, since it arises from a spherical wave originating from the sphere, E_0 is inversely proportional to the distance between the sphere and the detector (inverse square-law for the field intensity). If the detector is far from the scattering volume (compared to the volume's dimensions), the variations in the amplitude from spheres at different distances is negligible. Thus, if all spheres are identical (as in this experiment), and light at a single scattering angle is detected, E_0 can be taken as a constant for all spheres. However, the phase ϕ is very sensitive to the position of the sphere and can change by 2π as the sphere moves as little as a wavelength. Variations in ϕ as the spheres move are, in fact, the source of the intensity variations measured in this experiment.

To see how this comes about, we will first need an expression for the phase ϕ_j in terms of the position vector $\mathbf{r}_j$ of the jth sphere. We may arbitrarily take $\phi = 0$ for a sphere

at some arbitrarily chosen origin within the scattering volume (O in Fig. 1). Then, the phase of a wave from a sphere located at $\mathbf{r}_j$ would be $2\pi/\lambda$ (where λ is the wavelength in the medium) times the path length difference between a wave scattered from the origin and one scattered from $\mathbf{r}_j$. If the detector is far from the scattering volume V, the geometry is as shown in the lower part of Fig. 1 and gives

$$\phi_j = \frac{2\pi}{\lambda}(\overline{CPD} - \overline{AOB}) \qquad (30)$$

Exercise 5 *Show that the equation above can be rewritten*

$$\phi_j = (\mathbf{k}_i - \mathbf{k}_f) \cdot \mathbf{r}_j \qquad (31)$$

where $\mathbf{k}_i$ and $\mathbf{k}_f$ are the incident and scattered wavevectors, respectively.

The wavevector $\mathbf{k}_i$ points in the direction of the incident plane wave and $\mathbf{k}_f$ points in the direction of the outgoing waves (toward the detector) and both have the same magnitude

$$k = \frac{2\pi}{\lambda} \qquad (32)$$

where λ is the wavelength in the medium.

To do the exercise, redraw the figure and add perpendiculars from O to the line $\overline{CP}$ labeling the intersection point C' and from O to the line $\overline{PD}$ labeling the intersection point D'. The path length difference is then $\overline{C'P} + \overline{PD'}$. Then relate these two distances to $\mathbf{r}_j$ and the wavevectors $\mathbf{k}_i$ and $\mathbf{k}_f$.

Introducing the scattering vector $\mathbf{K}$,

$$\mathbf{K} = \mathbf{k}_i - \mathbf{k}_f \qquad (33)$$

ϕ_j can be written simply as

$$\phi_j = \mathbf{K} \cdot \mathbf{r}_j \qquad (34)$$

Exercise 6 *Draw a vector diagram showing the relationship between $\mathbf{k}_i$, $\mathbf{k}_f$ and $\mathbf{K}$ labeling the scattering angle θ between the incident and scattered wavevectors and show that the magnitude of $\mathbf{K}$ is given by*

$$K = 2k_i \sin\left(\frac{\theta}{2}\right) \qquad (35)$$

The total electric field is the sum of the electric field from all spheres

$$E(t) = \sum_{j=1}^{N} E_0 e^{i(\phi_j(t) - \omega_0 t)} \qquad (36)$$

where the sum is over all N illuminated spheres. The intensity $I(t)$ is proportional to the square of the electric field $I(t) = \beta|E(t)|^2 = \beta E(t)E^*(t)$

$$I(t) = \beta E_0^2 \sum_j \sum_k e^{i(\phi_j(t) - \phi_k(t))} \qquad (37)$$

Note that a time dependence has been added to ϕ_j in these equations. This is because the spheres randomly diffuse, and as $\mathbf{r}_j$ varies, so too do the ϕ_j—through Eq. 34. Thus $E(t)$ and $I(t)$ are random variables and cannot be explicitly determined.

This does not mean that we cannot obtain useful quantities related to the random variables $E(t)$ and $I(t)$. Two related quantities describing a variable which varies randomly in time are its power spectrum and its autocorrelation function.

The power spectrum of a time-varying signal $V(t)$ is defined in terms of the Fourier transform $\hat{V}(\omega)$ of $V(t)$

$$\hat{V}(\omega) = \int_{-\infty}^{\infty} V(t)e^{i\omega t}dt \qquad (38)$$

The power spectrum $S(\omega)$ is defined by

$$S_V(\omega) = \lim_{T \to \infty} \frac{1}{2T}\hat{V}(\omega)\hat{V}^*(\omega) \qquad (39)$$

The limiting procedure and the factor $1/2T$ arise because $V(t)$ is not square integrable.[2]

The autocorrelation function of a signal $V(t)$ is defined

$$R_V(\Delta t) = \lim_{T \to \infty} \frac{1}{2T} \int_{-T}^{T} V^*(t)V(t+\Delta t)dt \tag{40}$$

This is often written

$$R_V(\Delta t) = \langle V^*(t)V(t+\Delta t) \rangle \tag{41}$$

where the angle brackets indicate the time average given explicitly in the prior equation.

Thus $R_V(\Delta t)$ is the time average of the product of a signal with its value a time Δt later. For $\Delta t = 0$, it is the mean squared signal. $R_V(\Delta t)$ would decrease as Δt increases if the correlation of the signal with its value at later and later times decreases. Keep in mind that averaging times will need to be long—several minutes—to get good results in this experiment. However, the autocorrelation function will actually go to zero quickly—for $\Delta t \ll 1$ s.

Calculation of the Autocorrelation Function

The autocorrelation function for the intensity $I(t)$ would then be $R_I(\Delta t) = \langle I^*(t)I(t+\Delta t) \rangle$. With $I(t)$ given by Eq. 37 (and using rule 1 below) it becomes

$$R_I(\Delta t) = \beta^2 E_0^4 \sum_j \sum_k \sum_l \sum_m \tag{42}$$
$$\left\langle e^{-i(\phi_j(t)-\phi_k(t))} e^{i(\phi_l(t+\Delta t)-\phi_m(t+\Delta t))} \right\rangle$$

Note that

1. The average of a sum of terms is the sum of the average of each term.

---

2. The average of a product of terms is the product of the average of each term if each term is uncorrelated with the others.

3. The motion of one sphere is uncorrelated with the motion of any other sphere.

4. The average value of $e^{i\phi_j(t)}$ is zero because the sphere's move randomly over large distances compared to a wavelength within the averaging time.

Rule 4 is perhaps the most difficult and important to appreciate. According to Eq. 34 $\phi(t) = \mathbf{K} \cdot \mathbf{r}(t)$ and according to Eq. 35 the magnitude of $\mathbf{K}$ is on the order of $k_i = 2\pi/\lambda$. Over the averaging time, the particle wanders around in Brownian motion and its displacement $\mathbf{r}(t)$ moves through distances of many wavelengths λ. Consequently, $\phi(t)$ will vary through many cycles of 2π and because $e^{i\phi} = \cos\phi + i\sin\phi$, both its real and imaginary parts will vary through many oscillations. Finally, because the average of a sine or cosine function over many oscillations is zero, we get rule 4.

Rules 2-4 ensure that any $jklm$ term in Eq. 42 will time average to zero if one index is different from the other three. Thus, the only non-zero terms will be those in which pairs of indices are equal. There are three such cases: 1) $j = k$ and $l = m$, 2) $j = l$ and $k = m$, and 3) $j = m$ and $k = l$.

Letting N represent the number of illuminated spheres, there are N^2 pairs for case 1. With $j = k$ and $l = m$ it is easy to see that the exponential factor is unity for all of them.

There are $N^2 - N$ terms for case 2 where $j = l$ and $k = m$, but $j \neq k$. (the N terms with $j = k = l = m$ have already been counted in case 1). Each such term's exponential factor becomes

$$S_2 = \left\langle e^{-i(\phi_j(t)-\phi_j(t+\Delta t))} e^{i(\phi_k(t)-\phi_k(t+\Delta t))} \right\rangle \tag{43}$$

There are also $N^2 - N$ terms for case 3 where $j = m$ and $k = l$, but $j \neq k$, and each term's exponential factor becomes

$$S_3 = \left\langle e^{-i(\phi_j(t) + \phi_j(t + \Delta t))} e^{i(\phi_k(t) + \phi_k(t + \Delta t))} \right\rangle \tag{44}$$

Since different spheres' (j and k) motions are uncorrelated, the two exponential factors in S_2 and S_3 are independent and the average of their product is the product of their average. In both S_2 and S_3, the two factors are complex conjugates of one another giving

$$\begin{align} S_2 &= s_2 s_2^* \tag{45} \\ S_3 &= s_3 s_3^* \tag{46} \end{align}$$

where

$$\begin{align} s_2 &= \left\langle e^{-i(\phi(t) - \phi(t + \Delta t))} \right\rangle \tag{47} \\ s_3 &= \left\langle e^{-i(\phi(t) + \phi(t + \Delta t))} \right\rangle \tag{48} \end{align}$$

and the subscripting has been dropped as the average is over a single sphere.

Using Eq. 34 to substitute for each ϕ then gives

$$\begin{align} s_2 &= \left\langle e^{-i\mathbf{K} \cdot (\mathbf{r}(t) - \mathbf{r}(t + \Delta t))} \right\rangle \tag{49} \\ s_3 &= \left\langle e^{-i\mathbf{K} \cdot (\mathbf{r}(t) + \mathbf{r}(t + \Delta t))} \right\rangle \tag{50} \end{align}$$

We define

$$\Delta\mathbf{r}(t, \Delta t) = \mathbf{r}(t + \Delta t) - \mathbf{r}(t) \tag{51}$$

as the change in position or displacement of a sphere over the time interval from t to $t + \Delta t$. Using it to eliminate $\mathbf{r}(t + \Delta t)$ gives

$$\begin{align} s_2 &= \left\langle e^{i\mathbf{K} \cdot \Delta\mathbf{r}(t, \Delta t)} \right\rangle \tag{52} \\ s_3 &= \left\langle e^{i\mathbf{K} \cdot (2\mathbf{r}(t) + \Delta\mathbf{r}(t, \Delta t))} \right\rangle = 0 \tag{53} \end{align}$$

Note how $\mathbf{r}(t)$ cancels out in s_2 but not in s_3. Hence, the s_3 term is zero for the same reasons that justify rule 4. Rule 4 does not apply to s_2, however, because the variations in the exponent of that term are due to variations in $\Delta\mathbf{r}(t, \Delta t)$ which is the displacement of the particle from t to $t + \Delta t$. As one averages over the time t, $\Delta\mathbf{r}(t)$ will not vary over many wavelengths, at least not for small enough delay times Δt. If Δt is taken large enough, s_2 will, in fact, go to zero. However, this is precisely what this experiment is designed to determine.

The time average appearing in Eq. 52 is over a single particle's motion and if the complete trajectory were mapped out, that average (for one particular value of Δt and $\mathbf{K}$) would be obtained as follows. Pick the x-axis along the direction of $\mathbf{K}$ so that $\mathbf{K} \cdot \Delta\mathbf{r} = K\Delta x$. Make a list of the particle's x-coordinate x_0, x_1, ... at time steps t_0, t_1, ... spaced Δt apart throughout the time interval over which the averaging is to be performed. Find $\Delta x_1 = x_1 - x_0$, the x-displacement for the first time interval from t_0 to t_1 and evaluate $e^{iK\Delta x_1}$. Repeat this process to find the displacement Δx_2 for the second interval from t_1 to t_2 and evaluate $e^{iK\Delta x_2}$. Continue until you have covered the entire time interval. The average value of the $e^{iK\Delta x_i}$ is the sought after quantity.

$$s_2 = \frac{1}{N} \sum_{i=1}^{N} e^{iK\Delta x_i} \tag{54}$$

Can we predict this average? Because the particles undergo Brownian motion, the values of the Δx_i's appearing in Eq. 54 will be random variables. They will be distributed with probabilities governed by Eq. 23 (with the substitution of Δx for x and Δt for t in Eq. 22). As $N \to \infty$ the sample average in Eq. 54 can be calculated as a parent average—a weighted average over all possible Δx's with $dP(\Delta x)$ providing the weights. This gives

$$s_2 = \frac{1}{\sqrt{2\pi\sigma^2}} \int_{-\infty}^{\infty} e^{iK\Delta x} e^{-(\Delta x)^2 / 2\sigma^2} d\Delta x \tag{55}$$

We can expand $e^{iK\Delta x} = \cos K\Delta x +$

$i \sin K\Delta x$. The sine term gives an odd integrand over an even integration interval and therefore vanishes. The cosine term is easily integrated and gives

$$s_2 = e^{-K^2\sigma^2/2} \tag{56}$$

Now, we can write down an expression for $R_I(\Delta t)$. Recall that in the sum over j, k, l, m in Eq. 42, there are N^2 terms each contributing unity and $N^2 - N$ terms each contributing $s_2 s_2^* = e^{-K^2/\sigma^2}$. Thus,

$$R_I(\Delta t) = \beta^2 E_0^4 \left[N^2 + (N^2 - N)e^{-K^2\sigma^2} \right] \tag{57}$$

With $\sigma^2 = 2D\Delta t$ this equation predicts $R_I(\Delta t)$ will be a constant plus a decaying exponential

$$R_I(\Delta t) = A + Be^{-\Gamma\Delta t} \tag{58}$$

where the decay rate Γ would be given by

$$\Gamma = 2K^2D \tag{59}$$

Using Eqs. 28, 32 and 35 this becomes

$$\Gamma = \frac{32\pi n^2 k_B T}{3\eta\lambda_0^2} \cdot \frac{\sin^2(\theta/2)}{d} \tag{60}$$

where λ_0 is the vacuum wavelength and n is the medium's index of refraction ($\lambda = \lambda_0/n$).

Exercise 7 *The predicted decay rate given by Eq. 60 can be written*

$$\Gamma = \kappa \frac{\sin^2(\theta/2)}{d} \tag{61}$$

where κ is a function of the temperature T. Using $\lambda_0 = 632.8$ nm for the HeNe laser, $k_B = 1.3807 \times 10^{-23}$ J/K, and Table 1 for the index of refraction and viscosity of water, make a table and graph of κ in the temperature range $15 - 30°C$.

Temp. (°C)	η (kg/m/s)	n
15	0.001139	1.333
16	0.001109	1.333
17	0.001081	1.333
18	0.001053	1.333
19	0.001027	1.333
20	0.001002	1.333
21	0.000978	1.333
22	0.000955	1.333
23	0.000933	1.333
24	0.000911	1.333
25	0.000890	1.333
26	0.000871	1.332
27	0.000851	1.332
28	0.000833	1.332
29	0.000815	1.332
30	0.000798	1.332

Table 1: Values of the viscosity η and index of refraction n of pure water as a function of temperature T. (From *CRC Handbook of Chemistry and Physics*.)

Calculation of the Power Spectrum

The power spectrum for the intensity $I(t)$ and its Fourier transform $\hat{I}(\omega)$ are related by the reciprocal relationships

$$\hat{I}(\omega) = \int_{-\infty}^{\infty} I(t)e^{i\omega t}dt \tag{62}$$

and

$$I(t) = \int_{-\infty}^{\infty} \hat{I}^*(\omega)e^{-i\omega t}\frac{d\omega}{2\pi} \tag{63}$$

Using Eq. 63 to substitute for $I(t)$ and $I(t + \Delta t)$ in the expression for the autocorrelation function Eq. 40 gives

$$R_I(\Delta t) = \lim_{T\to\infty}\frac{1}{2T}\int_{-T}^{T}dt\int_{-\infty}^{\infty}\frac{d\omega}{2\pi}\int_{-\infty}^{\infty}\frac{d\omega'}{2\pi} \\ \left[\hat{I}(\omega)\hat{I}^*(\omega')e^{i\omega t}e^{-i\omega'(t+\Delta t)}\right] \tag{64}$$

Rearranging

$$R_I(\Delta t) = \frac{1}{2T} \int_{-\infty}^{\infty} \frac{d\omega}{2\pi} \int_{-\infty}^{\infty} \frac{d\omega'}{2\pi} \hat{I}(\omega)\hat{I}^*(\omega')$$

$$e^{-i\omega'\Delta t} \lim_{T\to\infty} \int_{-T}^{T} \left[e^{i(\omega-\omega')t} \right] dt \quad (65)$$

The last integral is a representation of the Dirac delta function

$$\lim_{T\to\infty} \int_{-T}^{T} e^{i(\omega-\omega')t} \, dt = 2\pi\delta(\omega - \omega') \quad (66)$$

giving

$$\begin{aligned} R_I(\Delta t) &= \lim_{T\to\infty} \frac{1}{2T} \int_{-\infty}^{\infty} \frac{d\omega}{2\pi} \int_{-\infty}^{\infty} \frac{d\omega'}{2\pi} \quad (67) \\ &\hat{I}(\omega)\hat{I}^*(\omega')e^{-i\omega'\Delta t}2\pi\delta(\omega - \omega') \end{aligned}$$

Noting that $\int_{-\infty}^{\infty} f(x)\delta(x - x_0)dx = f(x_0)$, the integration over ω' can be carried out giving

$$R_I(\Delta t) = \int_{-\infty}^{\infty} \left[\lim_{T\to\infty} \frac{1}{2T} \hat{I}(\omega)\hat{I}^*(\omega) \right] e^{-i\omega\Delta t} \frac{d\omega}{2\pi} \quad (68)$$

The term in square brackets is the definition (Eq. 39) of the intensity's power spectrum $S_I(\omega)$. Making this substitution gives

$$R_I(\Delta t) = \int_{-\infty}^{\infty} S_I(\omega)e^{-i\omega\Delta t} \frac{d\omega}{2\pi} \quad (69)$$

which shows that $R_I(\Delta t)$ and $S_I(\omega)$ form a Fourier transform pair. The reciprocal relation

$$S_I(\omega) = \int_{-\infty}^{\infty} R_I(\Delta t)e^{i\omega\Delta t}d\Delta t \quad (70)$$

allows us to predict the power spectrum from the autocorrelation function. Inserting Eq. 57 for $R_I(\Delta t)$ and performing the integration gives

$$S_I(\omega) = \beta^2(E_0)^4 \left[N^2 2\pi\delta(\omega) + \quad (71) \right.$$

$$\left. (N^2 - N)2(2DK^2)\frac{1}{\omega^2 + (2DK^2)^2} \right]$$
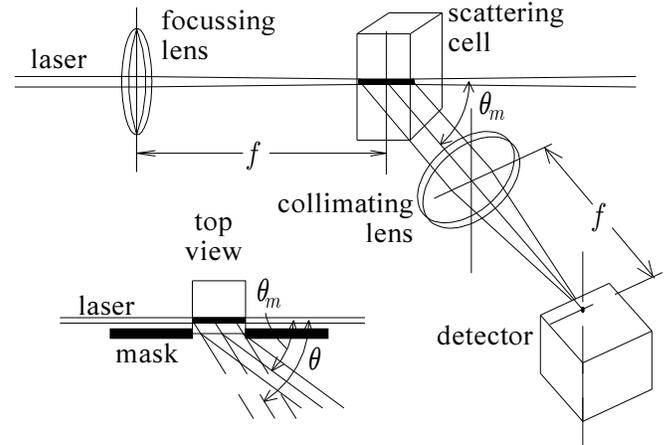

Figure 2: Upper figure: Experimental setup (aperture on collimating lens and cell mask not shown). Lower figure: Shows cell mask and refraction as light emerges from the cell.

Apart from the Dirac delta function, this expression is a Lorentzian centered at $\omega = 0$ and with Eq. 59 can be written in a form suitable for fitting purposes.

$$S_I(\omega) = A\delta(\omega) + \frac{B}{1 + (\omega/\Gamma)^2} \quad (72)$$

Apparatus

A schematic of the experiment is shown in Fig. 2. A HeNe laser is the source of the incident plane waves. (If, as in this experiment, the laser electric field is linearly polarized perpendicular to the scattering plane, so too is the scattered radiation.) The laser beam is focused to a sharp, horizontal line parallel to the wall of the scattering cell through which the scattered light will be observed. The scattered light passes through a lens and is detected by a small area (1 mm²) silicon avalanche photodiode detector placed at the focal point of the lens. This lens-detector arrangement ensures that all light impinging on the detector

emerged from the cell at nearly the same angle θ_m relative the original beam direction.

$I(t)$ includes a constant average scattering intensity that contains little relevant information. It affects the background level of the exponentially-decaying autocorrelation function and the DC component of the Lorentzian power spectrum, but does not affect Γ — the parameter of interest in this experiment. Γ is determined entirely by the variations in the intensity about its average value. In fact, the detector circuit (discussed next) includes an adjustment to offset this average intensity so we can better measure the intensity variations.

Detector

The silicon avalanche photodiode circuit is shown in Fig. 3. The detector reverse bias voltage V_d is supplied by an adjustable Kepco supply, while the positive and negative supplies for the operational amplifiers use the fixed ± 15 V supply. $V_d = 106$ V is specified by the manufacturer. Light of intensity $I(t)$ incident on the detector causes a proportional current $i(t)$ to flow through it. There is also an additional small dark current (background noise) associated with these detectors. The photocurrent $i(t)$ is converted to a voltage $v(t)$ by the first operational amplifier $v(t) = i(t)r$, where $r = 10$ MΩ. The 10kΩ potentiometer will need to be adjusted at each trial to offset the DC component of the intensity so that the analog-to-digital converter (ADC) in the computer can use the highest possible gain.

The variations in the detector signal $V(t)$ will be proportional to the intensity variations of the light incident on it. Thus, aside from the background level of $R_I(\Delta t)$ or the DC component of $S_I(\omega)$, the analysis for $I(t)$ is likewise true for $V(t)$.

The second op-amp is used in a two-pole Butterworth low-pass filter having its 3 dB fre-

quency set at $f_c = 1/2\pi RC$—around 7 kHz, with $R = 47$ kΩ and $C = 470$ pf. It also provides additional gain of about 47k/27k. The filter attenuates the high frequency components of the detector shot noise without appreciably decreasing the slower signal variations arising from the motion of the spheres.

Data sampling issues

The data acquisition program repeatedly acquires a finite sample of $I(t)$ at points equally spaced in time. You will specify the number of points N collected on each sample and the time interval t_s between points.

The autocorrelation function is then calculated from

$$R_I(\Delta t) = \langle I(t)I(t + \Delta t)\rangle \qquad (73)$$

for $\Delta t = i\,t_s$, $i = 0...N - 1$. The average is over all t for which pairs $I(t)$ and $I(t + \Delta t)$ exist in the sample.

Thus for $\Delta t = 0$ there are N pairs, for $\Delta t = t_s$ there are $N - 1$ pairs, ..., and for $\Delta t = (N - 1)t_s$ there is only a single pair (the first and last point in the sample). Thus for Δt near $(N - 1)t_s$ there will only be a few pairs in the average and the quality of these points will be poor.

There must be a reasonable number of points over the region of Δt where $R_I(\Delta t)$ is decaying exponentially. Thus t_s should be small compared to the time constant $1/\Gamma$ of the decay. The largest Γ you will measure will be around 1000/s and thus the shortest time for the exponential to completely decay (about 5 time constants) will be about 5 ms. Thus with the default value for t_s of 0.05 ms there will be at least 100 points in $R_I(\Delta t)$ over the first 5 time constants for even the fastest decays. With the default sample size of $N = 8192$, the first point $R_I(0)$ would be calculated with 8192 pairs while $R_I(5\,\text{ms})$ would
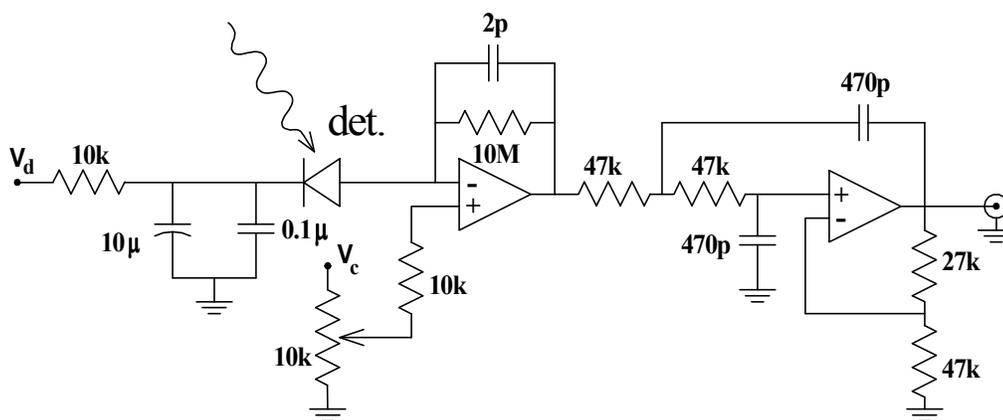
Figure 3: Avalanche photodiode (Hamamatsu S2382) detector circuit schematic. Positive and negative voltage supplies for the operational amplifiers (OP27) not shown.

use only slightly less (8093) pairs.[3]

The program also computes the power spectrum $S_I(\omega)$ (Eq. 39) using discrete Fourier transforms equivalent to Eq. 38. It is recommended that the sample size N be a power of two, such as 8192 ($= 2^{13}$), so that the fast-Fourier transform algorithm can be used. The power spectrum's Nyquist frequency[4] is half the sampling frequency and to prevent aliasing should be above the highest measurable frequencies. With the detector's 7 kHz low pass filtering, the default sampling rate of 20 kHz is a reasonable choice. The spacing between points in the power spectrum is the sampling frequency divided by the number of points in the sample. Using 8192 points at 20 kHz gives a frequency spacing of about 2.5 Hz. The Lorentzian component of the power spectrum is down to half its maximum value when $\omega = \Gamma$ or $f = \Gamma/2\pi$) and thus for the smallest Γ measured in this experiment (around 100/s), there

can be as few as 10-20 data points within one half-width.

The data acquisition program repeatedly takes an $I(t)$ sample, calculates $R_I(\Delta t)$ and $S_I(\omega)$, and then averages each of these functions point by point with the results from prior samples until data acquisition is stopped.

Procedure

Laser Safety

The helium neon laser has sufficient intensity to permanently damage your eye. Obviously, you must **never allow the laser beam to fall anywhere near your face.** Even a reflected beam can cause permanent eye damage. In fact, most accidents involving lasers are caused by reflections from smooth surfaces. To avoid such accidents the following steps must be taken.

1. Remove all reflective objects from your person (e.g., watches, shiny jewelry).

2. Make sure that you block all stray reflections coming from your experiment.

---

[3] The program that fits $R_I(\Delta t)$ to Eq. 58 weighs all data equally. For this to be a reasonable approximation, there should be approximately the same number of pairs for all points used in the fit.

[4]The Nyquist frequency is the highest frequency components accurately determined by a Fourier transform.

3. **Never be at eye level with the laser beam** (e.g., by leaning down).

4. Be careful when you change optics in your experiment so as not to inadvertently place a highly reflective object (mirror, post) into the beam.

The microspheres may clump together or, if the water is not distilled, particulates may begin to clump with the spheres. If you are in doubt as to the quality of your suspension, make a new one using one drop of sphere concentrate to a cell filled with distilled water. Add spheres or dilute further until a complete and bright scattering line is observed when the cell is illuminated by the laser beam.

You may need to de-clump samples before use (even newly-prepared samples) by holding the cell 1/2-3/4 submerged in the ultrasonic cleaner for 15-30 seconds. It's kind of neat to measure and fit the autocorrelation function (say at 90°) before and after to see if there is any effect from de-clumping.

Take a room temperature reading and use your results from *Exercise 7* to determine κ.

For each of the two sphere sizes:

1. Line up the sample cell, laser and focusing lens so that the laser beam makes a sharp line about 1 mm inside the front cell surface and so the illuminated line is centered over the pivot point of the detector arm.

2. Place a white screen downstream from the cell and observe the pattern of scattered light around the main spot and its temporal variations. Answer Comprehension Question 2

3. Using a polarizer, check the polarization of the laser. Make sure it is vertical for the rest of the experiment. But check out what happens when the laser is turned so that the polarization is horizontal. Answer Comprehension Question 3

4. Set the collimating lens/aperture as close as possible to the cell but far enough away so that it does not interfere with the arm's rotation. Mask the cell and set the aperture just wide enough to let in the light leaving the front of the cell, making sure that no light from the entrance or exit faces of the cell will be detected.

5. Position the detector one focal length from the collimating lens.

6. Connect the detector supply voltages and the detector output to the oscilloscope. Have the instructor check your connections before turning on the supplies.

7. Turn the room lights off and, if necessary, cover the apparatus with a dark cloth. Adjust the potentiometer to center the detector voltage around zero. (Check the zero level by temporarily grounding the scope input and making sure the scope is DC coupled.) Note the maximum amplitude of the noise signal from the detector.

8. Connect the detector output to the input labeled 1 on the interface box.

9. Launch the DLS data acquisition program and click on the run button in the LabVIEW toolbar if the program is not already running.

10. The input settings area has controls which determine various ADC conversion parameters. The input channel must correspond with the BNC input used on the interface box. The default values for the sample size and sampling rate were discussed earlier and should work well for all of the recommended measurements.

The range control for the ADC defaults to ±100 mV and should be set as small as possible compatible with the voltages from the detector, which can change depending on the scattering angle. Be sure to check that the measurements do not saturate. If the raw signal is flat or shows flattened out regions, the range control needs to be adjusted.

11. Click on the begin acquisition button and collect data until the autocorrelation function appears reasonably smooth. Then click on stop acquisition button. Note that any changes to the input settings do not affect a run in progress and only take effect when the begin acquisition button is pressed again.

12. Collect data for around 8 values of θ_m between about 30° to 120°, adjusting the input limits and the detector offset as appropriate for each signal. θ_m can be obtained by lining up the detector arm with the holes in the optical breadboard and taking an inverse tangent. Analyze each data set as described next.

Data analysis

Theoretically, even with the low pass filtering, shot noise from the detector is expected to modify the experimentally obtained $R_I(\Delta t)$ and $S_I(\omega)$. The shot noise is expected to add a $\delta(\Delta t)$ of some amplitude to $R_I(\Delta t)$ and a constant to $S_I(\omega)$. Recall there was already a predicted constant in $R_I(\Delta t)$ and a $\delta(\omega)$ in $S_I(\omega)$. Thus both should have a constant term and a Dirac delta function term (both of which are not important). To avoid dealing with the delta functions, make sure that the first point in each spectrum is not used in the fit. Thus the fitting function Eq. 58 is OK as it is and

the fitting function for $S_I(\omega)$ should be modified to

$$S_I(\omega) = A + \frac{B}{1 + (\omega/\Gamma)^2} \qquad (74)$$

i.e., we have dropped the delta function and added a constant term.

The graph of the processed signal can be changed to either the power spectrum or the autocorrelation function during or after data acquisition. If you accidentally stop the program, just hit the LabVIEW run button and the data should again be available although you will not be able to add to it. The curve fitting and save to spreadsheet features of the program work with the data selected for the graph.

After collecting a data set, select the autocorrelation function and then fit it to the prediction of Eq. 58 to determine best estimates of A, B and Γ. Note in the model description area below the graph how the name in the ind. var. and the names in the parameters array correspond with those used in the fitting model. Also note how the formula is written a+b*exp(-100*c*t). For our data sets, A and B are typically around one and Γ is typically several hundred. Recall that nonlinear fitting requires that you provide initial guesses for the fitting parameters and typically works better when all parameters are of the order unity. If the fit does not work properly, you may need to scale the fitting parameters to force them near unity. (Scaling is often the problem if one or more parameters do not change from their initial guesses.) This scaling technique is illustrated by the default fitting model which uses $\Gamma = 100c$ so that the fitting parameter c will be of order unity. If you scale the fitting parameters this way, remember to rescale them to get the actual physical parameters.

The cursors must be set to Lock to plot (the default) and the fit is performed only over the

region between the cursors displayed on the graph. The fitting program gives parameter uncertainty estimates, but they may not be reliable. You should vary the starting point (but never include the first point) and the ending point of the fit to get other estimates of the uncertainty in Γ. For example, try fitting the the first half of the decay curve and then the second half. Why might changing the fitting region affect the parameters? You should also check the reproducibility by repeating a few of the measurements and fits. Keep a record of the Γ's obtained so that you can make reasonable estimates of the best values and their uncertainties.

For one or two data sets try fitting the power spectrum to the prediction of Eq. 74. Keep in mind that the data for the power spectrum is intensity vs. frequency f (in Hz) while the prediction of Eq. 74 is expressed as a function of $\omega = 2\pi f$. For readability, you may want to change the ind. var. to f, even though it is simply a dummy variable. You might take care of the difference between f and ω by a fitting model such as $a + b/(1 + (f/(100 * c))^2)$ and demonstrating to yourself that in this case $\Gamma = 200\pi c$.

Compare the resulting Γ from this fit to value from the fit to the autocorrelation function. Should they give the same Γ?

If you want to try a fitting model with more than three parameters, all you need to do is name them in the parameters array, use them in the new fitting model, and supply initial guesses for them. If you want to try a one or two parameter fitting model, the process is the same, but you must first right click on the array index (the 0 at the top left of the array) for the parameters and initial guesses array and select Data Operations|Empty Array.

Because of the refraction at the cell wall, the true scattering angle θ and the measured angle θ_m will differ as demonstrated in the lower part of Fig. 2. Use Snell's law to deduce the relationship between them and determine θ for each θ_m used.

CHECKPOINT: You should have complete sets of measurements for each of the two samples of microspheres. An estimate of the microsphere diameter should be calculated from just the $\theta_m = 90°$ measurement to check if your data are reasonable.

Comprehension Questions

1. Explain qualitatively why Γ goes to zero at $\theta = 0$ and why it increases with increasing θ. As Γ increases, does the autocorrelation function decay faster or slower? As Γ increases, does the width (frequency content) of the power spectrum increase or decrease? Do these effects imply that the electric field changes more or less rapidly as Γ increases? Would this imply the same Brownian motion must result in faster or slower variations in E at larger scattering angles? Because the variations E are due to changes in the phase of the scattered waves as the particles move, we should check how the phase changes for a given particle motion. Thus, consider Fig. 1 (top). Assume that crests of the scattered wave are emitted as each crest from the incident plane wave hits the scatterer. The change in the scattered wave's phase at the detector will then be due to two possible effects. First, if the particle moves parallel to the *incident* wave direction there will be a corresponding change in the phase of the incident wave as it hits the scatterer, e.g., if the particle moves half a wavelength downstream, it will be hit by a crest half a period later compered to when it was

farther upstream. Secondly, if the particle moves parallel to the *scattered* wave direction, there will be a corresponding change in the phase of the scattered wave as it hits the detector, e.g., if the particle moves half a wavelength farther from the detector, the crests will hit the detector half a period later. So now consider figures like those of Fig. 1 for $\theta = 0$, $\pi/2$ and π. For each of the three scattering angles, explain how the phase at the detector for the wave scattered from a sphere at point P would change as the sphere moves a distance $\lambda/4$ (a) in the direction of $\mathbf{k}_i$ (to the right in the Fig. 1) and (b) perpendicular to that direction (say, down in Fig. 1). That's six cases all together. Finally, relate these cases to the original question.

2. Describe the pattern observed in the forward scattered light (viewed on the screen). As you move away from the central (unscattered) beam can you notice any systematic variations in the typical size of the bright spots in the pattern or in the speed at which they appear and disappear? Does this agree with your expectations? Explain.

3. When you turn the laser so the polarization is horizontal, what happens to the scattering light viewed at 90° to the beam direction? Explain your observations.

4. The measured signal has frequency components as described by Eq. 72. Note from the second term that as Γ increases the power spectrum spreads out to higher and higher frequencies. Since the filter cuts out frequencies above 7 kHz, determine the largest value of Γ for which the integral of the second term in Eq. 72 above 7 kHz is no more than 1% of the total integral. Which of your data sets will be most affected by the filtering? What fraction of the power is lost for this data set?

5. For each sample, plot Γ vs. $\sin^2(\theta/2)$. What does Eq. 60 predict for the shape of this plot? Perform a linear regression and find the slope and its uncertainty. Should the regression fit be forced through the origin? Explain. Check the rms deviation between the data and the fit and determine whether or not the results are in agreement with the predictions. Use your analysis with your value of κ and its uncertainty to determine the sphere diameters and their uncertainty. Compare with the manufacturer's stated value as given on the product sheets in the auxiliary material.